Rapidly Converging Spectral-Domain Analysis of Rectangularly Shielded Layered Microstrip Lines

John L. Tsalamengas and George Fikioris, *Member, IEEE*

***Abstract*—A moment-method-oriented direct integral-equation technique is presented for the exact analysis of rectangularly shielded layered microstrip lines. This technique retains the simplicity of conventional moment methods while optimizing them by recasting all matrix elements into rapidly converging series. Filling up the matrix requires no numerical integration. The proposed algorithms yield highly accurate results both for the modal currents and propagation constants.**

***Index Terms*—Analytical methods, microstrip lines, moment methods, spectral-domain analysis.**

I. Introduction

SPECTRAL-DOMAIN analysis (SDA) has been widely used for the investigation of microstrip structures [1]–[4]. Its remarkable simplicity in conjunction with the variational nature of the moment method (MoM) enables unsophisticated computation of the propagation constants with reasonable accuracy using a few basis functions. The required CPU time, however, rises extremely rapidly with accuracy. This occurs because it is necessary to compute several series that converge very slowly.

To overcome the problem of slow convergence of spectral series, several techniques have been used in the past. One such efficient technique is described in [5] and [6]. Accelerated versions of full-wave SDA are also developed in [7]–[9]. Finally, in [10], an efficient quasi-static analysis is presented, which can be used for speeding up full-wave computations as well. For the above reasons, the method of dual series equations (DSEs) [11] has been also used as a powerful alternative to the SDA; in particular, it can be used to obtain the characteristics of higher order modes [12]–[14]. In comparison with SDA, the method of the DSE is, however, rather multistage and cumbersome. More recently, a technique has been reported [15] for the extremely accurate SDA of generalized finlines, which recasts all spectral series involved into very rapidly convergent ones while retaining the simplicity of the conventional MoM. Although the techniques in [15] are unconventional, they yield very good results.

As pointed out in [6] and corroborated in [15] as well, the main difficulty with SDA is the accurate computation of the matrix elements and not matrix size. Motivated from this remark, the purpose of this paper is to extend the method of [15] to the case of a rectangularly shielded generalized microstrip line. This is carried out in Sections II–IV and, as in [15], leads to rapidly converging expressions for all matrix elements. As a result, extremely accurate results are obtainable with low computational cost as we demonstrate in Section V.

Planar microstrip structures have been studied for years, and the studies have led to computer programs (see, e.g., [16]) capable of providing results with sufficient accuracy for ordinary engineering applications. The aforementioned studies, and the ensuing computer programs, are general in the sense that they apply to a variety of geometries. The analysis herein only concerns the specific geometries mentioned above. However, as a result of the specialized nature of our analysis, we obtain results of very high accuracy using smaller-than-usual matrices. Our lower computational costs may be useful, for example, in discontinuity analysis problems, where the computation of many modes is required, or in optimization problems, where final designs are produced after a great number of candidate structures have been analyzed and compared. Furthermore, our results can also be used as benchmark tests for general-purpose computer programs. The present study, therefore, is not intended to compete with analyses leading to general-purpose computer programs and can, in fact, test and complement such programs.

II. Formulation

Shown in Fig. 1 is the geometry of a generalized microstrip line. The ith layer is characterized by the scalar constants ε_i, μ_i, and $k_i = \omega\sqrt{\varepsilon_i\mu_i}$. The strip, of width $2w$, is located at the interface ($y = 0$) between layers (1) and (-1). The two outmost regions can be occupied by a perfect electric conductor (PEC), a perfect magnetic conductor (PMC), or a dielectric; these outmost regions extend to infinity and are labeled ($-\ell - 1$) and ($p + 1$).

Assuming propagation in the $-\hat{z}$-direction and using the immittance approach [2], [17], the surface current density on the strip $\overline{J} = [J_x(x)\hat{x} + J_z(x)\hat{z}]e^{j(\omega t+\beta z)}$ is found to satisfy the system of integral equations (1) and (2), shown at the bottom of the following page. Here, we have adopted a notation similar to [15]: $C = \{x : c-w \le x \le c+w\}$ denotes the x-axis interval occupied by the strip, $\hat{\varepsilon}_n = 2 - \delta_{n0}$ is the Neumann's factor, and

$$k_x = \frac{n\pi}{a} \quad \psi_n(x) = \cos(k_x x) \quad \varphi_n(x) = \sin(k_x x). \tag{3}$$

The quantities Ψ^e and Ψ^h in (1) and (2) are given by

$$\Psi^q = \sum_{s=-1,1} Y^q(h_s) \tag{4}$$

Manuscript received October 4, 2002; revised January 29, 2003. This work was supported by the Institute of Communication and Computer Systems of the National Technical University of Athens under Archimedes 2000-01 Basic Research Project 65/37.

The authors are with the Department of Electrical and Computer Engineering, National Technical University of Athens, Zografou 157-73, Athens, Greece.

Digital Object Identifier 10.1109/TMTT.2003.812576

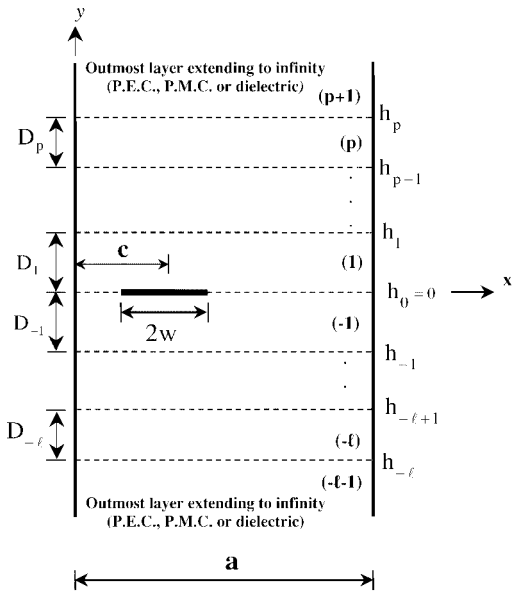

Fig. 1. Geometry of the problem.

where $Y^q(h_1)\backslash Y^q(h_{-1})$ are evaluated recursively downwards\upwards from

$$Y^q(h_{i\mp1}) = y_i^q \frac{Y^q(h_i) \pm y_i^q \tanh(\gamma_i D_i)}{y_i^q \pm Y^q(h_i)\tanh(\gamma_i D_i)} \tag{5}$$

with starting values $Y^q(h_p) = y_{p+1}^q$, $Y^q(h_{-l}) = -y_{-l-1}^q$, respectively, where

$$\begin{aligned} y_i^e &= \frac{-j\omega\varepsilon_i}{\gamma_i} \\ y_i^h &= -\frac{j\gamma_i}{\omega\mu_i} \end{aligned} \tag{6}$$

$$\begin{aligned} \gamma_i^2 &= \beta^2 + k_x^2 - k_i^2 = k_x^2 - \kappa_i^2 \\ \kappa_i^2 &\equiv k_i^2 - \beta^2 \quad \left(0 \le \arg(\gamma_i) \le \frac{\pi}{2}\right). \end{aligned} \tag{7}$$

III. Discretization of (1) and (2) by Conventional SDA

We change variables $x = c + wt$, $x' = c + w\tau$ ($-1 \le t, \tau \le 1$) and expand

$$\begin{aligned} J_z[x'(\tau)] &= \frac{1}{\sqrt{1-\tau^2}} \sum_{N=0}^{\infty} a_N T_N(\tau) \\ J_x[x'(\tau)] &= \sqrt{1-\tau^2} \sum_{N=0}^{\infty} b_N U_N(\tau) \end{aligned} \tag{8}$$

where T_N and U_N are the Chebyshev polynomials. In accordance with conventional MoM, we insert from (8) into (1) and (2) and take the inner product with $T_M(t)/\sqrt{1-t^2}$ and with $\sqrt{1-t^2}U_M(t)$ ($M = 0, 1, 2, \ldots$) to obtain

$$\sum_{n=0}^{\infty} (a_N K_{\mathrm{MN}}^{\mathrm{zz}} + b_N K_{\mathrm{MN}}^{\mathrm{zx}}) = 0 \tag{9a}$$

$$\sum_{N=0}^{\infty} \left[a_N K_{\mathrm{MN}}^{\mathrm{xz}} + b_N \left(-\frac{\pi^2 w}{4a\Psi^h|_{n=0}} \delta_{M0}\delta_{N0} + K_{\mathrm{MN}}^{\mathrm{xx}} \right) \right] = 0, \qquad M = 0, 1, 2, \ldots, \infty. \tag{9b}$$

The matrix elements are given by

$$\begin{aligned} K_{\mathrm{MN}}^{\mathrm{zz}} &= K_{\mathrm{MN}}^{\mathrm{zz}}(\Psi^h, \Psi^e) = \frac{\pi^2}{a} w j^{M+N} \\ &\quad \cdot \sum_{n=1}^{\infty} \frac{1}{k_x^2 + \beta^2} \left(\frac{k_x^2}{\Psi^h} - \frac{\beta^2}{\Psi^e} \right) g_{M,N}(n) \end{aligned} \tag{10a}$$

$$\begin{aligned} -K_{\mathrm{NM}}^{\mathrm{xz}} &= K_{\mathrm{MN}}^{\mathrm{zx}} = K_{\mathrm{MN}}^{\mathrm{zx}}(\Psi^h, \Psi^e) = \frac{\pi^2}{a} j^{M+N} \beta (N+1) \\ &\quad \cdot \sum_{n=1}^{\infty} \frac{1}{k_x^2 + \beta^2} \left(\frac{1}{\Psi^h} + \frac{1}{\Psi^e} \right) g_{M,N+1}(n) \end{aligned} \tag{10b}$$

$$\begin{aligned} K_{\mathrm{MN}}^{\mathrm{xx}} &= K_{\mathrm{MN}}^{\mathrm{xx}}(\Psi^h, \Psi^e) = -\frac{a}{w} j^{M+N} (M+1)(N+1) \\ &\quad \cdot \sum_{n=1}^{\infty} \frac{1}{n^2} \frac{1}{k_x^2 + \beta^2} \left(\frac{\beta^2}{\Psi^h} - \frac{k_x^2}{\Psi^e} \right) g_{M+1,N+1}(n) \end{aligned} \tag{10c}$$

where

$$g_{M,N}(n) = J_M\left(\frac{n\pi w}{a}\right) J_N\left(\frac{n\pi w}{a}\right) \cdot \begin{cases} -(-1)^M + \cos\left(\dfrac{2n\pi c}{a}\right), & M+N \text{ even} \\ j\sin\left(\dfrac{2n\pi c}{a}\right), & M+N \text{ odd.} \end{cases} \tag{11}$$

In (11), $J_M(\cdot)$ is the Bessel function of order M. It is readily verified that all series in (10) converge rather slowly, as n^{-2}. As a result, it is extremely difficult to achieve high accuracy using (10). In the following section, these difficulties are faced head on by recasting all matrix elements into rapidly converging series following methods similar to those in [15] and [18].

$$E_z(x,0) \equiv -\frac{2}{a} \sum_{n=1}^{\infty} \frac{\varphi_n(x)}{k_x^2 + \beta^2} \left[-j\beta k_x \left(\frac{1}{\Psi^h} + \frac{1}{\Psi^e} \right) \int_C J_x(x')\psi_n(x')dx' + \left(\frac{k_x^2}{\Psi^h} - \frac{\beta^2}{\Psi^e} \right) \int_C J_z(x')\varphi_n(x')dx' \right] = 0 \tag{1}$$

$$E_x(x,0) \equiv -\frac{1}{a} \sum_{n=0}^{\infty} \frac{\psi_n(x)}{k_x^2 + \beta^2} \left[\hat{\varepsilon}_n \left(\frac{\beta^2}{\Psi^h} - \frac{k_x^2}{\Psi^e} \right) \int_C J_x(x')\psi_n(x')dx' + 2j\beta k_x \left(\frac{1}{\Psi^h} + \frac{1}{\Psi^e} \right) \int_C J_z(x')\phi_n(x')dx' \right] = 0, \quad x \in C. \tag{2}$$

IV. Improved SDA

Let

$$\Psi^q = y_1^q + y_{-1}^q + Q^q(n). \tag{12}$$

then

$$Q^q(n) = \sum_{\substack{s=-1,1 \\ q\equiv e,h}} s y_s^q \frac{Y^q(h_s) - s y_s^q}{y_s^q + s Y^q(h_s)\tanh(\gamma_s D_s)} \frac{2}{1+\exp(2\gamma_s D_s)}, \tag{13}$$

decay very strongly (exponentially) as $n \to \infty$. Using (12), one obtains

$$\frac{1}{\Psi^q} = \frac{1}{y_1^q + y_{-1}^q} + P^q \tag{14}$$

where

$$P^q(n) = -\frac{1}{y_1^q + y_{-1}^q} \frac{Q^q(n)}{Y^q(0+) - Y^q(0-)} \tag{15}$$

decay exponentially with increasing n. In view of (14), we have the result

$$K_{\rm MN}^{\rm ij}(\Psi^h, \Psi^e) = K_{\rm MN}^{\rm ij}\left(\frac{1}{P^h}, \frac{1}{P^e}\right) + \tilde{K}_{\rm MN}^{\rm ij}, \qquad i,j \equiv x,z \tag{16}$$

where

$$\tilde{K}_{\rm MN}^{\rm ij} \equiv K_{\rm MN}^{\rm ij}\left(y_1^h + y_{-1}^h, y_1^e + y_{-1}^e\right). \tag{17}$$

As seen, the computation of $K_{\rm MN}^{\rm ij}(1/P^h, 1/P^e)$ $(i,j \equiv x,z)$ via (10) involves very strongly (exponentially) converging series solely and is, thus, very efficient. Therefore, our main objective henceforth will be the efficient evaluation of the quantities $\tilde{K}_{\rm MN}^{\rm ij} \equiv K_{\rm MN}^{\rm ij}(y_1^h + y_{-1}^h, y_1^e + y_{-1}^e)$ $(i,j \equiv x,z)$ of (17), whose series expressions (10) continue to converge very slowly (as n^{-2}).

A. Acceleration of $\tilde{K}_{\rm MN}^{\rm ij}$ $(i,j \equiv x,z)$

After some algebraic manipulations, one may obtain the results

$$\frac{1}{y_1^h + y_{-1}^h} + \frac{1}{y_1^e + y_{-1}^e} = \frac{j}{\omega\varepsilon_1}(k_x^2 + \beta^2)[\xi_1 f_\mu + \xi_2 f_\varepsilon] \tag{18}$$

$$\frac{\beta^2}{y_1^h + y_{-1}^h} - \frac{k_x^2}{y_1^e + y_{-1}^e} = -\frac{j}{\omega\varepsilon_1}(k_x^2 + \beta^2) \cdot \left[(\xi_1 f_\mu + \xi_2 f_\varepsilon)k_x^2 - k_1^2 \mu f_\mu\right] \tag{19}$$

$$\frac{k_x^2}{y_1^h + y_{-1}^h} - \frac{\beta^2}{y_1^e + y_{-1}^e} = -\frac{j}{\omega\varepsilon_1}(k_x^2 + \beta^2)(\xi_3 f_\mu + \xi_2 \beta^2 f_\varepsilon) \tag{20}$$

where

$$\begin{aligned} \xi_1 &= \frac{1-\mu^2}{\varepsilon - \mu} \\ \xi_2 &= \frac{\varepsilon\mu - 1}{\varepsilon - \mu} \\ \xi_3 &= \frac{1}{\varepsilon - \mu}(\mu^2\kappa_1^2 - \kappa_{-1}^2) \end{aligned} \tag{21}$$

$$\begin{aligned} \mu &\equiv \frac{\mu_{-1}}{\mu_1} \\ \varepsilon &\equiv \frac{\varepsilon_{-1}}{\varepsilon_1} \end{aligned} \tag{22}$$

$$\begin{aligned} f_\mu &= f_\mu(n) \equiv \frac{1}{\gamma_{-1} + \mu\gamma_1} \\ f_\varepsilon &= f_\varepsilon(n) \equiv \frac{1}{\gamma_{-1} + \varepsilon\gamma_1}. \end{aligned} \tag{23}$$

In addition, one can verify that

$$f_u = \frac{A_u}{\gamma_1} + \frac{B_u}{\gamma_1 + \gamma_{-1}} + F_u, \qquad u \equiv \varepsilon, \mu \tag{24}$$

where

$$\begin{aligned} A_u &\equiv \frac{u-1}{(u+1)^2} \\ B_u &\equiv \frac{4}{(u+1)^2} \end{aligned} \tag{25}$$

$$F_u = F_u(n) \equiv -A_u \frac{(k_1^2 - k_{-1}^2)^2}{\gamma_1(\gamma_1 + \gamma_{-1})^3(\gamma_{-1} + u\gamma_1)}. \tag{26}$$

As seen, $F_u(n)$ decay as n^{-5} for large values of n.

Using these results, $\tilde{K}_{\rm MN}^{\rm ij}$ can be written as the sum of two terms

$$\tilde{K}_{\rm MN}^{\rm ij} = \frac{j}{\omega\varepsilon_1}\left(R_{\rm MN}^{\rm ij} + T_{\rm MN}^{\rm ij}\right), \qquad i,j \equiv x,z. \tag{27}$$

The first term in (27) involves $R_{\rm MN}^{\rm ij}$, which is given by

$$R_{\rm MN}^{\rm zz} = -\frac{\pi^2}{a} w j^{M+N} \sum_{n=1}^{\infty} \left[\xi_3 F_\mu(n) + \xi_2 \beta^2 F_\varepsilon(n)\right] g_{M,N}(n) \tag{28a}$$

$$-R_{\rm NM}^{\rm xz} = R_{\rm MN}^{\rm zx} = \frac{\pi^2}{a} j^{M+N} \beta (N+1) \sum_{n=1}^{\infty} \left[\xi_1 F_\mu(n) + \xi_2 F_\varepsilon(n)\right] g_{M,N+1}(n) \tag{28b}$$

$$R_{\rm MN}^{\rm xx} = \frac{a}{w} j^{M+N}(M+1)(N+1) \cdot \sum_{n=1}^{\infty} \frac{1}{n^2} \left\{ \left[\xi_1 F_\mu(n) + \xi_2 F_\varepsilon(n)\right] k_x^2 - k_1^2 \mu F_\mu(n) \right\} \cdot g_{M+1,N+1}(n). \tag{28c}$$

We observe that all series in (28) converge as $1/n^6$, i.e., very rapidly. Therefore, the computation of $R_{\rm MN}^{\rm ij}$ via (28) is very efficient. Note also that the rate of convergence of these series can be easily improved to any order, if desired, by extracting high-order asymptotic terms from F_ε and F_μ.

The second term in (27) involves $T_{\rm MN}^{\rm ij}$. If $G_{M,N}^{(\pm 1)}$, $\hat{G}_{M,N}^{(\pm 1)}$, $\Lambda_{M,N}$, and $\hat{\Lambda}_{M,N}$ denote the series

$$G_{M,N}^{(\pm 1)} = \sum_{n=1}^{\infty} \frac{1}{\gamma_{\pm 1}} g_{M,N}(n) \tag{29a}$$

$$\hat{G}_{M,N}^{(\pm 1)} = \sum_{n=1}^{\infty} \frac{1}{n^2 \gamma_{\pm 1}} g_{M,N}(n) \tag{29b}$$

$$\Lambda_{M,N} = \sum_{n=1}^{\infty} \frac{1}{\gamma_1 + \gamma_{-1}} g_{M,N}(n) \tag{29c}$$

$$\hat{\Lambda}_{M,N} = \sum_{n=1}^{\infty} \frac{1}{n^2} \frac{1}{\gamma_1 + \gamma_{-1}} g_{M,N}(n) \tag{29d}$$

then the quantities $T_{\rm MN}^{\rm ij}$ in (27) are given by

$$T_{\rm MN}^{\rm zz} = -\frac{\pi^2}{a} w j^{M+N} \Big[(\xi_3 A_\mu + \xi_2 \beta^2 A_\varepsilon) G_{M,N}^{(1)} + (\xi_3 B_\mu + \xi_2 \beta^2 B_\varepsilon) \Lambda_{M,N} \Big] \tag{30a}$$

$$-T_{\rm NM}^{\rm xz} = T_{\rm MN}^{\rm zx} = \frac{\pi^2}{a} j^{M+N} \beta (N+1) \cdot \Big[(\xi_1 A_\mu + \xi_2 A_\varepsilon) G_{M,N+1}^{(1)} + (\xi_1 B_\mu + \xi_2 B_\varepsilon) \Lambda_{M,N+1} \Big] \tag{30b}$$

$$T_{\rm MN}^{\rm xx} = \frac{a}{w} j^{M+N} (M+1)(N+1) \cdot \left\{ \left(\frac{\pi}{a}\right)^2 \Big[(\xi_1 A_\mu + \xi_2 A_\varepsilon) G_{M+1,N+1}^{(1)} + (\xi_1 B_\mu + \xi_2 B_\varepsilon) \Lambda_{M+1,N+1} \Big] - k_1^2 \mu (A_\mu \hat{G}_{M+1,N+1}^{(1)} + B_\mu \hat{\Lambda}_{M+1,N+1}) \right\}. \tag{30c}$$

The first and third series in (29) converge as n^{-2} (i.e., very slowly), the second and fourth as n^{-4}. All these series can be accelerated to any order by the techniques described below, which resemble the techniques of [18].

B. Acceleration of $G_{M,N}^{(1)}$ and $\hat{G}_{M,N}^{(1)}$

We rewrite $G_{M,N}^{(\pm 1)}$ and $\hat{G}_{M,N}^{(\pm 1)}$ as

$$G_{M,N}^{(\pm 1)} = \Gamma_{M,N}^{(k)} + \Big[G_{M,N}^{(\pm 1)} - \Gamma_{M,N}^{(k)} \Big] \tag{31}$$

$$\hat{G}_{M,N}^{(\pm 1)} = \hat{\Gamma}_{M,N}^{(k)} + \Big[\hat{G}_{M,N}^{(\pm 1)} - \hat{\Gamma}_{M,N}^{(k)} \Big] \tag{32}$$

where the kth order asymptotic expressions $\Gamma_{M,N}^{(k)}$, $\hat{\Gamma}_{M,N}^{(k)}$ of $G_{M,N}^{(\pm 1)}$, and $\hat{G}_{M,N}^{(\pm 1)}$ are given by

$$\left\{ \begin{matrix} \Gamma_{M,N}^{(k)} \\ \hat{\Gamma}_{M,N}^{(k)} \end{matrix} \right\} = \frac{a}{\pi} \sum_{m=0}^{k} \frac{(2m-1)!!}{(2m)!!} \left(\frac{\kappa_{\pm 1} a}{\pi}\right)^{2m} \left\{ \begin{matrix} P_{M,N}^{(2m+1)} \\ P_{M,N}^{(2m+3)} \end{matrix} \right\} \tag{33}$$

in which

$$P_{M,N}^{(2m+1)} = \sum_{n=1}^{\infty} \frac{1}{n^{2m+1}} g_{M,N}(n) = -(-1)^M L_{\rm MN}^{(2m+1)} + U_{\rm MN}^{(2m+1)} + j V_{\rm MN}^{(2m+1)}. \tag{34}$$

Exponentially converging series expressions for $L_{\rm MN}^{(2m+1)}$, $U_{\rm MN}^{(2m+1)}$, and $V_{\rm MN}^{(2m+1)}$ are given in [18]. The quantities $[G_{M,N}^{(\pm 1)} - \Gamma_{M,N}^{(k)}]$ and $[\hat{G}_{M,N}^{(\pm 1)} - \hat{\Gamma}_{M,N}^{(k)}]$ in (31) and (32) are given by series that converge, respectively, as n^{-2k-4} and n^{-2k-6}, i.e., very strongly. (For instance, if we select to use the second-order acceleration scheme ($k = 2$), then the series convergence is n^{-8} and n^{-10}, respectively).

C. Acceleration of $\Lambda_{M,N}$ and $\hat{\Lambda}_{M,N}$

Using the relation

$$\frac{1}{n^2} \frac{1}{\gamma_1 + \gamma_{-1}} = \frac{1}{n^2} \frac{\gamma_1 - \gamma_{-1}}{\gamma_1^2 - \gamma_{-1}^2} = \frac{1}{n^2} \frac{\gamma_1 - \gamma_{-1}}{\kappa_{-1}^2 - \kappa_1^2} = \frac{1}{n^2 (\kappa_{-1}^2 - \kappa_1^2)} \left(\frac{\gamma_1^2}{\gamma_1} - \frac{\gamma_{-1}^2}{\gamma_{-1}} \right) \tag{35}$$

in conjunction with (7), we get the results

$$\hat{\Lambda}_{\rm MN} = \frac{1}{\kappa_{-1}^2 - \kappa_1^2} \cdot \left[\left(\frac{\pi}{a}\right)^2 (G_{\rm MN}^{(1)} - G_{\rm MN}^{(-1)}) - \kappa_1^2 \hat{G}_{\rm MN}^{(1)} + \kappa_{-1}^2 \hat{G}_{\rm MN}^{(-1)} \right] \tag{36}$$

$$\Lambda_{\rm MN} = \frac{1}{\kappa_{-1}^2 - \kappa_1^2} \left[-\kappa_1^2 G_{\rm MN}^{(1)} + \kappa_{-1}^2 G_{\rm MN}^{(-1)} + \left(\frac{\pi}{a}\right)^2 \Theta_{\rm MN} \right]. \tag{37}$$

The quantity $\Theta_{\rm MN}$ in (37) is given by the following series:

$$\Theta_{\rm MN} = \sum_{n=1}^{\infty} n^2 \left(\frac{1}{\gamma_1} - \frac{1}{\gamma_{-1}} \right) g_{\rm MN}, \tag{38}$$

which converges as n^{-2}. This series can be accelerated to any order k ($k = 0, 1, 2, \ldots$) by recasting as

$$\Theta_{\rm MN} = [\Theta_{\rm MN} - H_{\rm MN}^{(k)}] + H_{\rm MN}^{(k)} \tag{39}$$

where

$$H_{\rm MN}^{(k)} = \frac{a}{\pi} \sum_{m=1}^{k} \frac{(2m-1)!!}{(2m)!!} \left[\left(\frac{\kappa_1 a}{\pi}\right)^{2m} - \left(\frac{\kappa_{-1} a}{\pi}\right)^{2m} \right] P_{M,N}^{(2m-1)}. \tag{40}$$

The series for $[\Theta_{\rm MN} - H_{\rm MN}^{(k)}]$ is rapidly converging, whereas $P_{M,N}^{(2m-1)}$, defined by (34), can be evaluated by exponentially converging series as outlined above.

Note: It is important to note that the basic quantities $P_{M,N}^{(2m-1)}$, defined in (34) and used in (33) and (40), are independent of the unknown propagation constant β and, therefore, need only be evaluated once at the beginning. This feature greatly adds to the efficiency of the algorithm.

V. Numerical Results and Comparisons

A. Convergence Versus Matrix Size

For several matrix sizes, Table I shows the normalized propagation constants of the first five modes supported by the structure of Fig. 2 for the parameter values $\varepsilon_r = 8.875$, $\mu_r = 1$, $fr = 20$ GHz, $a = 12.7$ mm, $c = 0.5$ a, $2w = 0.1$ a, $D_1 = 11.43$ mm, $D_2 = 1.27$ mm, and $k = 2$ (second-order

TABLE I
β/k_0 OF THE FIRST FIVE MODES OF THE STRUCTURE OF FIG. 2

	Mode No:				
Matrix size	1	2	3	4	5
4×4	2.710834747119	1.289217957341	1.102710850613	0.9223125840602	0.7251113444022
6×6	2.710205697853	1.289495579763	1.102636555234	0.9223133626275	0.7250995972107
8×8	2.710205800947	1.289452731573	1.102636604307	0.9223133479505	0.7250996003284
10×10	2.710205710947	1.289452746771	1.102636588906	0.9223133480852	0.7250996002924
12×12	2.710205710951	1.289452745015	1.102636588908	0.9223133480797	0.7250996002924
14×14	2.710205710950	1.289452745015	1.102636588907	0.9223133480797	0.7250996002924
16×16	2.710205710950	1.289452745015	1.102636588907	0.9223133480796	0.7250996002924
18×18	2.710205710950	1.289452745015	1.102636588907	0.9223133480796	0.7250996002924
[13] 20×20	2.70975	1.28682	1.10136	0.921501	0.724452
[13] 30×30	2.71001	1.28692	1.10140	0.921503	0.724453

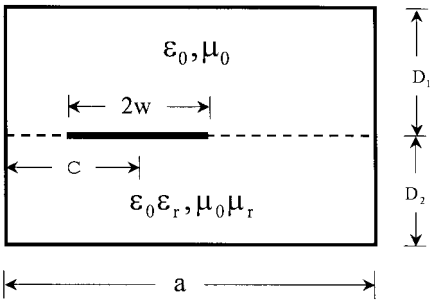

Fig. 2. Single-layered microstrip line.

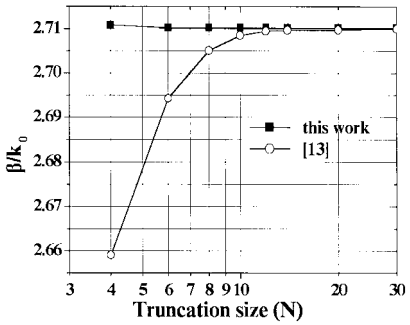

Fig. 3. Convergence of β/k_0 for the first mode versus N (the matrix size is $N \times N$), and comparison with [14].

acceleration). As seen, the convergence of our algorithm versus matrix size is very stable and rapid. For instance, a 6×6 matrix (use of three basis functions for each of J_x and J_z) suffices in most cases to obtain an accuracy to within seven significant figures, whereas for a 12×12 matrix, the accuracy reaches 12 significant figures.

In order to test the correctness of our algorithm, Table I also contains results taken from [14] based on the DSE method for 20×20 and 30×30 matrices. The agreement is very good for all modes. We further observe that, in comparison with [14], our results reach their final values for considerably smaller matrix sizes. Illustrative in this respect is Fig. 3, based on Table I and on [14, Table I], which compares the rapidity of convergence versus N ($N \times N$ denotes the matrix size) between this work and [14]. As seen from this figure, the values of [14] asymptotically approach our plot, which is almost horizontal.

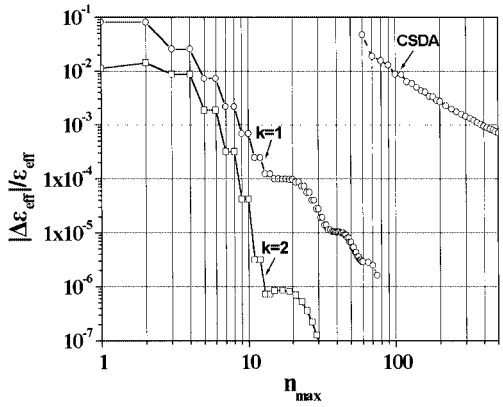

Fig. 4. Relative error $\Delta\varepsilon_{\text{eff}}/\varepsilon_{\text{eff}}$ versus the number of series terms (structure of Fig. 2: $\varepsilon_r = 11.7$, $\mu_r = 1$, $fr = 4$ GHz, $a = 34.74$ mm, $c = 0.5$ a, $2w = 3.04$ mm, $D_1 = 50$ mm, and $D_2 = 3.17$ mm).

B. Convergence Versus the Number of Series Terms

As noted above, the proposed algorithm enables one to compute all matrix elements via rapidly converging series. To illustrate this very important feature, we first truncate all infinite series involved by retaining only $n_{\max}$ terms in each of them. In Fig. 4, we then show the relative error $\Delta\varepsilon_{\text{eff}}/\varepsilon_{\text{eff}}$ versus $n_{\max}$, where $\Delta\varepsilon_{\text{eff}} = |\varepsilon_{\text{eff}}(n_{\max}) - \varepsilon_{\text{eff}}|$, with $\varepsilon_{\text{eff}} = \varepsilon_{\text{eff}}(n_{\max} \to \infty) = 8.8100416$ denoting the exact value of the effective dielectric constant (see below). Here, we refer to the structure of Fig. 2 for the parameter values $\varepsilon_r = 11.7$, $\mu_r = 1$, $fr = 4$ GHz, $a = 34.74$ mm, $c = 0.5$ a, $2w = 3.04$ mm, $D_1 = 50$ mm, and $D_2 = 3.17$ mm. Six basis functions are used in each of (8).

As seen from Fig. 4, both our first- and second-order algorithms (curves labeled "$k = 1$" and "$k = 2$," respectively) yield a rapidly decaying error with increasing $n_{\max}$. When $k = 2$, for instance, even for $n_{\max} = 1$, the relative error $\Delta\varepsilon_{\text{eff}}/\varepsilon_{\text{eff}}$ is less than 0.011 (or 1.1%). For $n_{\max} = 9$, this error is only 1.23×10^{-5}, whereas for $n_{\max} = 31$, it becomes 6.86×10^{-8}. In contrast, the conventional SDA (curve labeled "CSDA") is seen to be very slowly converging (due to series converging as $1/n^2$, as we noted above).

C. Further Results

Very accurate results (to within eight figures) for the microstrip line have been recently reported in [6]. Thus, to

TABLE II
ε_{eff} FOR $n_{\max} = 40, 70$ AND FOR SEVERAL MATRIX SIZES $N \times N$. THE PARAMETER VALUES ARE THE SAME AS IN FIG. 4

	ε_{eff}	
N×N	$n_{\max}$=40	$n_{\max}$=70
4×4	8.8114918	8.8114916
6×6	8.8100416	8.8100414
8×8	8.8100418	8.8100417
10×10	8.8100417	8.8100416
12×12	8.8100417	8.8100416
14×14	8.8100417	8.8100416
Value accurate to within 12 figures: ε_{eff}=8.81004157493 (for $n_{\max}$=260)		
From [6]: ε_{eff}=8.8100416		

further test and appreciate the efficiency and accuracy of our algorithm, Table II presents values of the effective dielectric constant pertaining to the structure of Fig. 2 for two values of $n_{\max}$ and for several matrix sizes when the parameter values are selected as in Fig. 4. As seen, our results coincide with those of [6]. Of course, by further increasing $n_{\max}$, the accuracy can be improved even more. When $n_{\max} = 260$, for instance, results accurate to within 12 figures are obtained ($\varepsilon_{\text{eff}} = 8.81004157493$).

VI. CONCLUSION

The highly accurate evaluation of the propagation constants in rectangularly shielded generalized microstrip lines is a difficult task in the context of the conventional MoM. The difficulties, which are due to the slowly convergent series in the expressions for the matrix elements, have been faced head on in this paper by recasting all matrix elements into rapidly converging series using analytical acceleration techniques resembling those in [15] and [18]. With the help of the algorithm proposed herein, the MoM is optimized, while its simplicity is retained. These new algorithms are promising alternatives to other multistage and cumbersome methods such as the dual series technique used in the past.

REFERENCES

[1] N. G. Alexopoulos, "Integrated-circuit structures on anisotropic substrates," *IEEE Trans. Microwave Theory Tech.*, vol. MTT-33, pp. 847–881, Oct. 1985.

[2] T. Itoh, *Numerical Techniques for Microwave and Millimeter-Wave Passive Structures*. New York: Wiley, 1989.

[3] R. H. Jansen, "The spectral-domain approach for microwave integrated circuits," *IEEE Trans. Microwave Theory Tech.*, vol. MTT-33, pp. 1043–1056, Oct. 1985.

[4] ——, "A comprehensive CAD approach to the design of MMICs up to MM-wave frequencies," *IEEE Trans. Microwave Theory Tech.*, vol. 36, pp. 208–219, Feb. 1988.

[5] G. Cano, F. Mesa, F. Medina, and M. Horno, "Systematic computation of the modal spectrum of boxed microstrip, finline, and coplanar waveguides via an efficient SDA," *IEEE Trans. Microwave Theory Tech.*, vol. 43, pp. 866–872, Apr. 1995.

[6] G. Cano, F. Medina, and M. Horno, "On the efficient implementation of SDA for boxed strip-like and slot-like structures," *IEEE Trans. Microwave Theory Tech.*, vol. 46, pp. 1801–1806, Nov. 1998.

[7] C. J. Railton and J. P. McGeehan, "A rigorous and computationally efficient analysis of microstrip for use as an electro-optic modulator," *IEEE Trans. Microwave Theory Tech.*, vol. 37, pp. 1099–1104, July 1989.

[8] J.-W. Tao, G. Angenieux, and B. Flechet, "Full-wave description of propagation and losses in quasiplanar transmission lines by quasianalytical solution," *IEEE Trans. Microwave Theory Tech.*, vol. 42, pp. 1246–1253, July 1994.

[9] G. Cano, F. Medina, and M. Horno, "Efficient spectral domain analysis of generalized microstrip lines in stratified media including thin, anisotropic and lossy substrates," *IEEE Trans. Microwave Theory Tech.*, vol. 40, pp. 217–227, Feb. 1992.

[10] F. Medina and M. Horno, "Quasianalytical static solution of the boxed microstrip line embedded in a layered medium," *IEEE Trans. Microwave Theory Tech.*, vol. 40, pp. 1748–1756, Sept. 1992.

[11] L. Lewin, "The use of singular integral equations in the solution of waveguide problems," in *Advances in Microwaves*, L. Young, Ed. New York: Academic, 1966, vol. 1, pp. 212–284.

[12] R. Mittra and T. Itoh, "A new technique for the analysis of the dispersion characteristics of microstrip lines," *IEEE Trans. Microwave Theory Tech.*, vol. MTT-19, pp. 47–56, Jan. 1971.

[13] A. S. Omar and K. Schunemann, "Formulation of the singular integral equation technique for planar transmission lines," *IEEE Trans. Microwave Theory Tech.*, vol. MTT-33, pp. 1313–1321, Dec. 1985.

[14] Y.-S. Xu and A. S. Omar, "Rigorous solution of mode spectra for shielded multilayer microstrip lines," *IEEE Trans. Microwave Theory Tech.*, vol. 42, pp. 1213–1222, July 1994.

[15] J. L. Tsalamengas, "Rapidly converging spectral-domain analysis of shielded layered finlines," *IEEE Trans. Microwave Theory Tech.*, vol. 47, pp. 805–810, June 1999.

[16] R. H. Jansen, *MCLINE Computer Program*. Aachen, Germany: MCAD Software + Design Corporation, 1984, pp. 1–20.

[17] T. Itoh, "Spectral domain immittance approach for calculating the dispersion characteristics of microstrip lines," *IEEE Trans. Microwave Theory Tech.*, vol. MTT-28, pp. 733–736, July 1980.

[18] J. L. Tsalamengas, "A parallel plate-fed slot antenna loaded by a dielectric semi cylinder," *IEEE Trans. Antennas Propagat.*, vol. 44, pp. 1031–1040, July 1996.

John L. Tsalamengas, photograph and biography not available at time of publication.

George Fikioris (S'90–M'94), photograph and biography not available at time of publication.